LncRNA MIR4435-2HG inhibits the progression of osteoarthritis through miR-510-3p sponging

YINGLI LIU[1*], YUN YANG[2*], LIANGJIA DING[2], YUQIN JIA[3] and YUNTAO JI[4]

[1]Rehabilitation Center, The Second Affiliated Hospital of Inner Mongolia Medical University, Hohhot, Inner Mongolia 010000; Departments of [2]Joint Surgery, [3]ICU (Intensive Care Unit) and [4]Education office, The Second Affiliated Hospital of Inner Mongolia Medical University, Hohhot, Inner Mongolia 010030, P.R. China

Received December 2, 2019; Accepted April 17, 2020

DOI: 10.3892/etm.2020.8841

Abstract. Osteoarthritis (OA) is a disorder of diarthrodial joints that can have multiple causes. Long non-coding RNAs (lncRNAs) participate in multiple diseases, including OA. It has recently been reported that the lncRNA microRNA 4435-2HG (MIR4435-2HG) is downregulated in OA tissues; however, the biological role of MIR4435-2HG during OA progression remains unclear. In the present study, interleukin (IL)-1β was used to establish an *in vitro* model of OA. Protein expressions of matrix metallopeptidase (MMP) 1, MMP13, collagen II, interleukin (IL)-17A, p65, phosphorylated (p)-p65, IκB and p-IκB in CHON-001 cells were detected by western blotting. Gene expressions of IL-17A, MIR4435-2HG and miR-510-3p in tissues or CHON-001 cells were measured by reverse transcription-quantitative PCR and western blotting, respectively. Cell Counting Kit-8 assay and immunofluorescence staining were used to investigate cell proliferation, and cell apoptosis was detected by flow cytometry. The association between MIR4435-2HG, miR-510-3p and IL-17A was investigated using the dual luciferase report assay. MIR4435-2HG and miR-510-3p overexpression were transfected into CHON-001 cells. The results demonstrated that miR4435-2HG overexpression significantly increased proliferation and inhibited apoptosis of CHON-001 cells. In addition, miR-510-3p was identified as the downstream target of MIR4435-2HG, and miR-510-3p directly targeted IL-17A. The results from the present study suggested that MIR4435-2HG could mediate the progression of OA by inactivating the NF-κB signaling pathway. In addition, miR4435-2HG overexpression inhibited OA progression, suggesting that miR4435-2HG may be considered as a potential therapeutic target in OA.

Correspondence to: Dr Liangjia Ding, Department of Joint Surgery, The Second Affiliated Hospital of Inner Mongolia Medical University, 1 Yingfang Road, Hohhot, Inner Mongolia 010030, P.R. China
E-mail: liangjiading8374@126.com

*Contributed equally

Key words: osteoarthritis, microRNA-4435-2HG, microRNA-510-3p, interleukin-17A

Introduction

Osteoarthritis (OA) affects ~50 million adults in China, and the currently available treatment strategies only manage pain (1,2). OA leads to the breakdown and gradual loss of joint cartilage, triggering debilitating pain and subsequent disability (3). The disease mainly affects the aging population, and >37% of individuals aged 60 years or older are affected by OA (4). At present, arthroscopic surgery and painkiller therapy are the main treatment options for OA; however, these treatment strategies result in 36,000,000 ambulatory care visits and 750,000 hospitalizations annually (5,6), leading to a high socioeconomic burden (7). Identifying new treatment strategies for OA is therefore important.

An increasing number of studies reported that non-coding RNAs (ncRNAs) are possible mediators of cell proliferation (8,9). ncRNAs are defined as transcripts of >200 nucleotides in length with limited or no protein-coding capacity, which are referred to as long non-coding RNAs (lncRNAs) (10). lncRNAs serve crucial roles in multiple diseases (11). For example, Jiang *et al* (12) reported that the lncRNA heart and neural crest derivatives expressed 2-antisense RNA1 inhibits 5-fluorouracil resistance by modulating the microRNA (miR)-20a/programmed cell death 4 axis in colorectal cancer. Furthermore, Li *et al* (13) reported that the Pvt1 oncogene regulates chondrocyte apoptosis in OA by acting as a miR-488-3p sponge. In addition, Xiao *et al* (14) demonstrated that the lncRNA MIR4435-2HG is downregulated in OA and can mediate chondrocyte proliferation and apoptosis. However, the role of miR4435-2HG during the progression of OA remains unknown. The present study aimed therefore to investigate the biological function of MIR4435-2HG in OA *in vitro*.

Materials and methods

Tissue collection. OA cartilage tissues (taken from patients with OA) and normal cartilage tissues (n=20 in each group) were collected from patients at the Second Affiliated Hospital of Inner Mongolia Medical University between February 2019 and June 2019. Clinicopathological characteristics were also

collected from these patients who provided written informed consent. Patients were diagnosed with OA according to The American College of Rheumatology classification criteria for the diagnosis of OA (15). The present study was approved by the Institutional Ethical Committee of the Second Affiliated Hospital of Inner Mongolia Medical University. Patient characteristics are presented in Table I. Normal tissues were collected from patients who have suffered from traffic accidents. These patients provided written informed consent. Collected tissues were stored at -80˚C until further use.

Cell culture. The human chondrocyte cell line CHON-001 and 293T cells were obtained from the American Type Culture Collection. Cells were cultured in RPMI-1640 medium (Invitrogen; Thermo Fisher Scientific, Inc.) supplemented with 10% fetal bovine serum (Invitrogen; Thermo Fisher Scientific, Inc.) and 2 mM glutamine (Sigma-Aldrich; Merck KGaA) andplaced at 37˚C in a humidified incubator containing 5% CO_2. CHON-001 cells were treated with 10 ng/ml interleukin (IL)-1β (Sigma-Aldrich; Merck KGaA) at room temperaturefor 24 h to generate an *in vitro* model of OA (16). The nuclear factor κB (NF-κB) inhibitor BAY 11-7085 (10 μM) was purchased from MedChemExpress.

Cell transfection. 293T cells ($5x10^6$/well) were transfected with 1 μg/μl pLVX-IRES-Puro-MIR4435-2HG overexpression (OE) vector or pLVX-IRES-Puroempty vector (both from Shanghai GenePharma Co., Ltd.) using Lipofectamine® 3000 reagent (Invitrogen; Thermo Fisher Scientific, Inc.) according to the manufacturer's protocol. The helper packaging vectors (pLP/VSVG, pLP1 and pLP2) were obtained from Invitrogen, Thermo Fisher Scientific, Inc., and used at a concentration of 1 μg/μl. After transfection, cells were incubated at 32˚C for 48 h. Subsequently, the 293T lentiviral supernatant containing the retroviral particles, was collected following centrifugation at 4˚C, 956 x g for 15 min.

For transduction, supernatant was passed through a 45-μm filter (Costar; Corning, Inc.) to obtain viral particles, which were then added to CHON-001 cells. After transduction for 48 h, cells were selected with puromycin (Sigma-Aldrich; Merck KGaA). The knockdown efficiency was verified by reverse transcription-quantitative PCR (RT-qPCR).

RT-qPCR. Total RNA was extracted from tissues or CHON-001 cells using TRIzol® reagent (Invitrogen; Thermo Fisher Scientific, Inc.) according to the manufacturer's protocol. Total RNA was reverse transcribed into cDNA using the PrimeScript RT reagent kit (Takara Bio, Inc.) according to the manufacturer's protocol. Subsequently, RT-qPCR was performed using the SYBR premix Ex Taq II kit (Takara Bio, Inc.) according to the manufacturer's protocol. All reactions were performed in triplicate as follows: 2 min at 94˚C, followed by 35 cycles at 94˚C for 30 sec and 55˚C for 45 sec. The sequences of the primes used for RT-qPCR were as follows: MIR4435-2HG forward, 5'-GGAAGTGGT GGCTATGAGTCAG-3' and reverse, 5'-TGTCAATTTGAA ACTTAAAAAGCAG-3'; IL-17A forward, 5'-CTACAACCG ATCCACCTCACC-3' and reverse, 5'-AGCCCACGGACA CCAGTATC-3'; β-actin forward, 5'-GTCCACCGCAAATGC TTCTA-3' and reverse, 5'-TGCTGTCACCTTCACCGTTC-3'; U6 forward, 5'-CTCGCTTCGGCAGCACAT-3' and reverse 5'-AACGCTTCACGAATTTGCGT-3'. miRNA and mRNA expression levels were quantified using the $2^{-\Delta\Delta Cq}$ method (17) and normalized to the internal reference genes β-actin or U6.

Cell Counting Kit-8 (CCK-8) assay. The CCK-8 assay (Beyotime Institute of Biotechnology) was used to assess cell proliferation according to the manufacturer's protocol. CHON-001 cells were plated in 96-well plates at a density of $5x10^3$ cells/well and treated for 0, 24, 48 or 72 h at 37˚C. The cells were cultured with 10 ng/ml IL-1β alone, MIR4435-2HG OE lentivirus alone, or both (IL-1β + MIR4435-2HG OE). Subsequently, CHON-001 cells were incubated with 10 μl CCK-8 reagent for 2 h at 37˚C. The absorbance was measured at a wavelength of 450 nm using a microplate reader (Thermo Fisher Scientific, Inc.).

Western blotting. Total protein was extracted from cell lines using RIPA lysis buffer (Beyotime, Institute of Biotechnology). Total protein was quantified using abicinchoninic acid protein kit (Thermo Fisher Scientific, Inc.). Protein (40 μg per lane) was separated by SDS-PAGE on 10% gels and transferred to PVDF membranes (Thermo Fisher Scientific, Inc.). Subsequently, the membranes were blocked with 5% skimmed milk in TBST for 1 h at room temperature. The membranes were incubated overnight at 4˚C with primary antibodies against collagen II (cat. no. ab239007), matrix metalloproteinase (MMP)-1 (cat. no. ab118973), MMP13 (cat. no. ab219620), IL-17A (cat. no. ab136668), p65 (cat. no. ab16502), inhibitor of κB (IκB; cat. no. ab109330), p-p65 (cat. no. ab6503), p-IκB (cat. no. ab225650) and β-actin (cat. no. ab179467). All primary antibodies were purchased from Abcam and diluted at 1:1,000. Following primary incubation, membranes were incubated with HRP-conjugated secondary antibodies (Abcam; cat. no. ab20272, 1:5,000) for 1 h at room temperature. Protein bands were visualized using the ECL kit (Thermo Fisher Scientific, Inc.). β-actin was used as the loading control. The Image-Pro Plus version 6 0 software was used for densitometry analysis.

Immunofluorescence. CHON-001 cells were cultured in 24-well plates overnight at the density of $5x10^4$ cells/well. Cells were pre-fixed with 4% paraformaldehyde at room temperature for 10 min and fixed in pre-cooled methanol at 4˚C for another 10 min. Subsequently, cells were incubated overnight at 4˚C with a primary antibody against Ki67 (1:1,000; cat. no. ab270650; Abcam). Following primary incubation, cells were incubated with a goat anti-rabbit IgG (HRP-conjugated) antibodies (1:5,000; ab125900, Abcam) at room temperature for 1 h. Cells were observed using a CX23 fluorescence microscope (magnification, x200; Olympus Corporation).

Cell apoptosis analysis. CHON-001 cells were seeded in 6-well plates at a density of $5x10^4$ cells/well and cultured for 48 h. CHON-001 cells were centrifuged at 15 x g for 5 min (at 4˚C), and the pellet was resuspended in 100 μl binding buffer. Subsequently, 5 μl Annexin V-fluorescein isothiocyanate and 5 μl propidium iodide were added to the cells for 15 min at 4˚C. Samples were analyzed by flow cytometry

Table I. Clinical characteristics of patients with osteoarthritis and healthy controls.

Clinical characteristics	Healthy, n	Patients, n	P-value
Age, years	48±8	52±10	0.786
Sex			
Male	17	18	0.821
Female	13	12	0.678
BMI, kg/m^2	23.7±2.1	24.1±2.5	0.788

BMI, Body Mass Index.

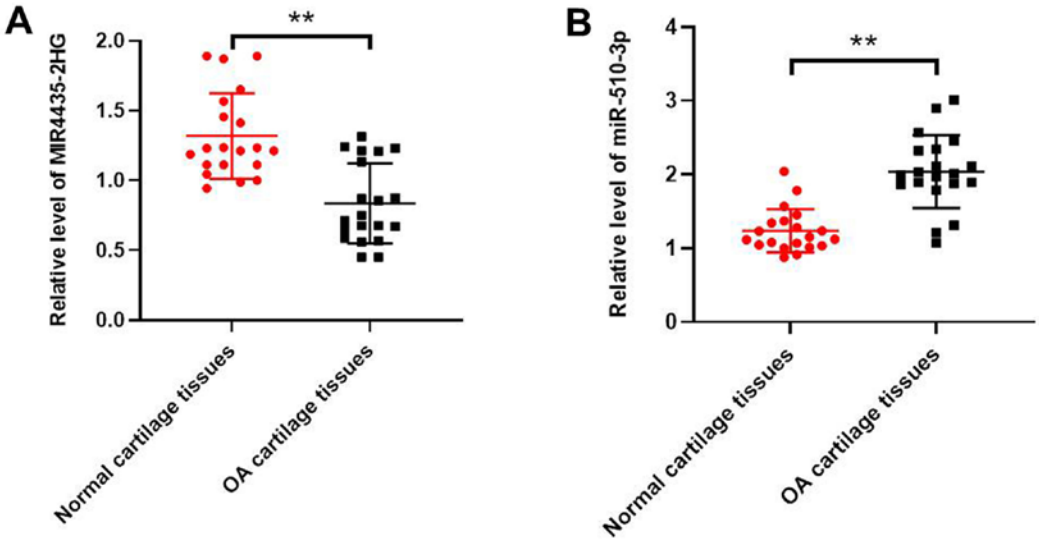

Figure 1. MIR4435-2HG was downregulated in OA tissues. (A) Expression levels of MIR4435-2HG in human OA tissues or normal tissues were detected using RT-qPCR. β-actin was used as an internal control. (B) Expression levels of miR-510-3pin OA and normal tissues were detected using RT-qPCR. U6 was used as an internal control. **P<0.01 vs. normal group. OA, osteoarthritis; miR, microRNA; RT-qPCR, reverse transcription-quantitative PCR.

(BD Biosciences) and apoptotic cells were analyzed using the WinMDI software version 2.9 (Invitrogen; Thermo Fisher Scientific, Inc.).

Downstream target genes prediction. Downstream target genes of MIR4435-2HG were predicted by using the publicly available program Starbase 2.0 (http://starbase.sysu.edu.cn/). In addition, miR-526b-3p targeted gene prediction was performed using two publicly available programs, TargetScan 7.2 (www.targetscan.org/vert_71/) and miRDB 4.0 (www.mirdb.org). The results obtained from Starbase were considered to be the downstream target genes of MIR4435-2HG. The resulting data of TargetScan 7.2 and miRDB 4.0 were selected as the direct gene of miR-526b-3p.

Dual luciferase reporter assay. The partial sequences of MIR4435-2HG and the IL-17A 3'-untranslated region (UTR) containing the putative binding sites of miR-510-3p were provided by Sangon Biotech Co., Ltd. The sequences were cloned into the pmirGLO Dual-Luciferase miRNA Target Expression Vectors (Promega Corporation) to construct wild-type (WT) reporter MIR4435-2HG and IL-17A vectors. The mutant (MUT) MIR4435-2HG sequence and IL-17A 3'-UTR containing the putative binding sites of miR-510-3p were generated using the Q5 Site-Directed Mutagenesis kit (New England Biolabs, Inc.) according to the manufacturer's protocol. The aforementioned MUT sequences were cloned into pmirGLO vectors to construct MUT reporter MIR4435-2HG and IL-17A vectors. The WT or MUT MIR4435-2HG vectors were transfected into CHON-001 cells together with control (untransfected cells), 10 nM vector-control (pcDNA-3.1 vector, Beyotime) or 10 nM miR-510-3p mimic using Lipofectamine® 2000 reagent (Thermo Fisher Scientific, Inc.) for 48 h, according to the manufacturer's instructions (blank group means untransfected cells; vector control group means cells transfected with pcDNA-3.1 vector). The sequence of the miR-510-3p mimic was as follows: 5'-AAUCCUUUGUCCCUGGGUGAGA-3'. The sequence of mimic negative control was as follows: 5'-UCACAACCUCCUAGAAAGAGUAGA-3'. Similarly, the WT and MUT IL-17A vectors were transfected into 293T cells together with control, vector-control or miR-510-3p mimics using Lipofectamine 2000 for 48 h. Relative luciferase activities were detected using a Dual-Glo Luciferase assay system (Promega Corporation). The data were normalized to *Renilla* luciferase activity.

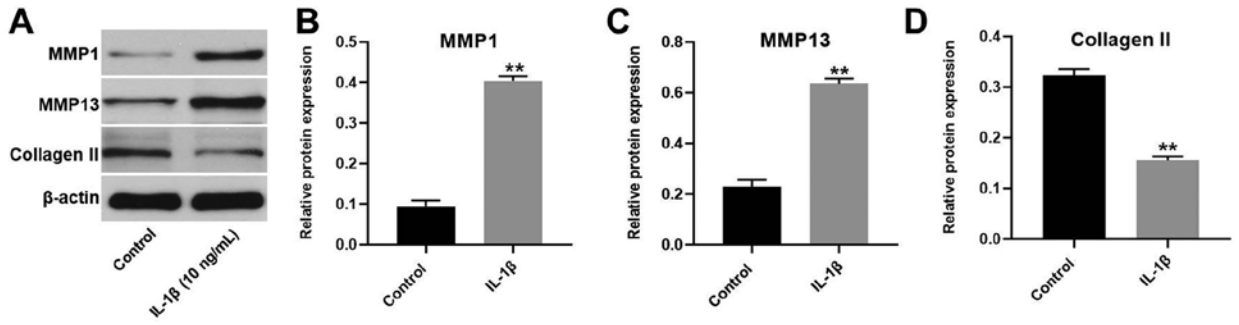

Figure 2. Establishment of an *in vitro* model of osteoarthritis. CHON-001 cells were treated with 10 ng/ml IL-1β for 24 h. (A) Expressions of MMP1, MMP13 and collagen II in CHON-001 cells were detected by western blotting. (B) Relative protein expression of MMP1 was normalized to β-actin. (C) Relative protein expression of MMP13 was normalized to β-actin. (D) Relative protein expression of collagen II was normalized to β-actin. **P<0.01 vs. control. MMP, matrix metalloproteinase; IL-1β. IL, interleukin.

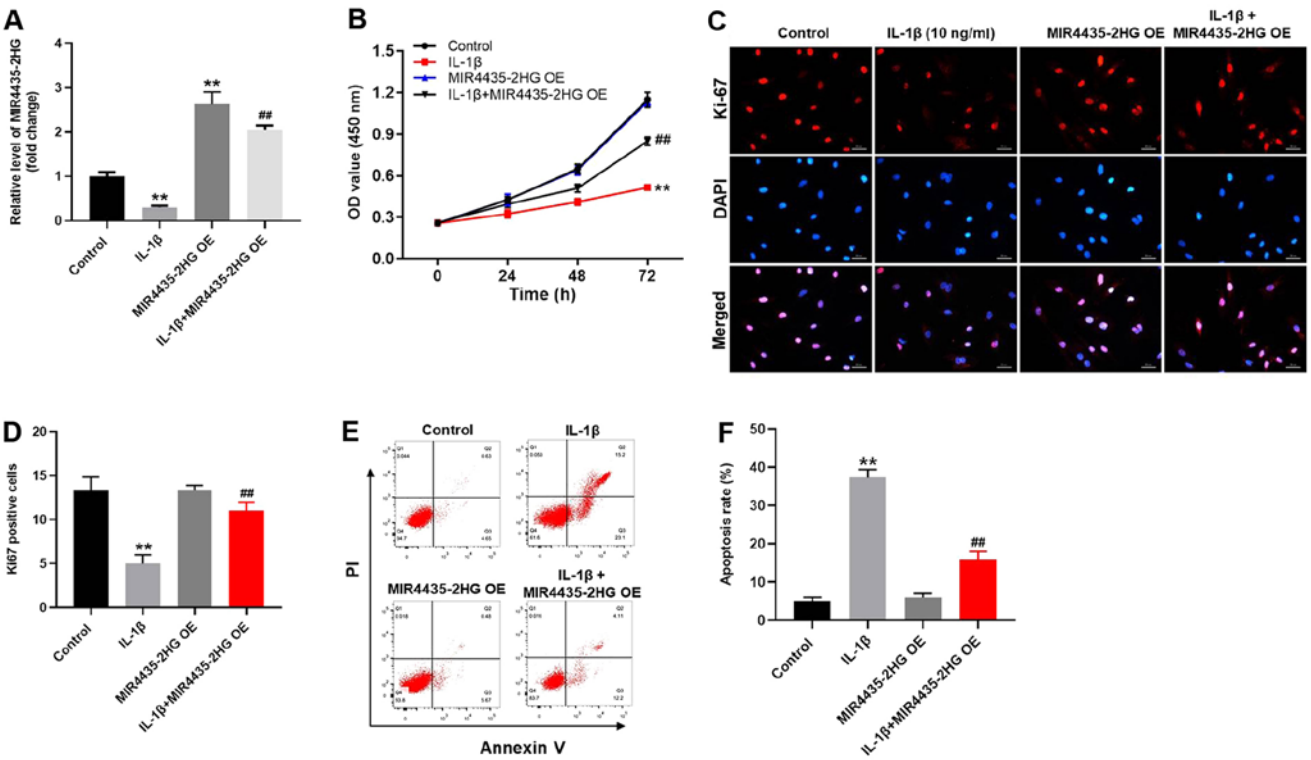

Figure 3. MIR4435-2HG OE promoted the growth of IL-1β-treated CHON-001 cells. Cells were treated with empty vector (control), IL-1β, MIR4435-2HG OE vector or IL-1β+ MIR4435-2HG OE. (A) Expression of MIR4435-2HG in CHON-001 cells was detected by reverse transcription-quantitative PCR. (B) OD values were measured in CHON-001 cells after0, 24 and 48 h using Cell Counting Kit-8 assay. (C and D) Proliferation of CHON-001 cells was assessed by Ki-67 staining. Red immunofluorescence indicated Ki-67. Blue immunofluorescence indicated DAPI. (E and F) CHON-001 cells were doubled stained with Annexin V and PI. Cell apoptosis was measured by flow cytometry. **P<0.01 vs. control; $^{\#\#}$P<0.01 vs. IL-1β. OE, overexpression; IL, interleukin; PI, propidium iodide; OD, optical density.

Statistical analysis. Data were presented as the means ± standard deviation. Comparison between two groups was analyzed by the Student's t-test. Multi-group comparison was analyzed using one-way ANOVA followed by Tukey's post hoc test. Statistical analysis was conducted using GraphPad Prism version 7 (GraphPad Software, Inc.). P<0.05 was considered to indicate a statistically significant difference.

Results

MIR4435-2HG is downregulated andmiR-510-3p is upregulated in OA tissues. Expression levels of MIR4435-2HG and miR-510-3p were determined in OA and normal tissues using RT-qPCR. As indicated in Fig. 1A, MIR4435-2HG expression level was significantly downregulated in OA tissues compared with normal tissues. However, the expression level of miR-510-3p was significantly up regulated in OA tissue compared with normal tissue (Fig. 1B).

Establishment of an in vitro model of OA. To establish an *in vitro* model of OA, CHON-001 cells were treated with 10 ng/ml IL-1β (Fig. 2). The expression of MMP1 and MMP13 in CHON-001 cells was significantly increased following IL-1β treatment. However, the expression of collagen II was

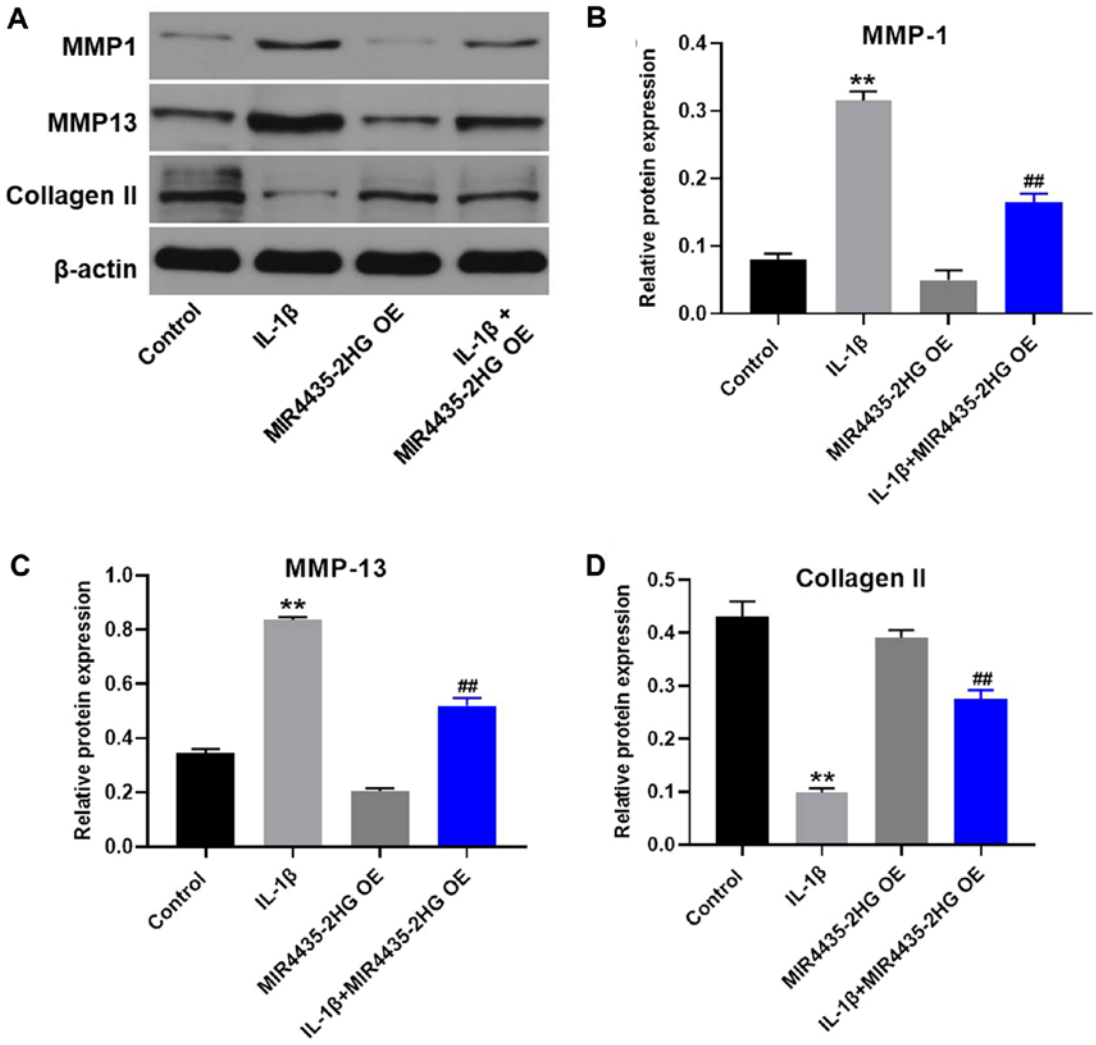

Figure 4. MIR4435-2HG OE downregulated MMP1 and MMP13 and upregulated collagen II in IL-1β-treated CHON-001 cells. (A) Protein expression of MMP-1, MMP13 and collagen II in CHON-001 cells was detected by western blotting. (B) Relative protein expression of MMP1 was normalized to β-actin. (C) Relative protein expression of MMP13 was normalized to β-actin. (D) Relative protein expression of collagen II was normalized to β-actin. **P<0.01 vs. control; $^{\#\#}$P<0.01 vs. IL-1β. OE, overexpression; IL, interleukin; MMP, matrix metalloproteinase.

significantly decreased in CHON-001 cells. Since these three proteins are key markers of OA (18), the results suggested that the *in vitro* model of OA had been successfully established.

MIR4435-2HG OE significantly promotes the proliferation of CHON-001 cells treated with IL-1β. To investigate the gene expression, RT-qPCR was performed (Fig. 3A). The expression level of MIR4435-2HG in CHON-001 cells was significantly decreased following IL-1β treatment (Fig. 3A). However, MIR4435-2HG expression was increased following transfection with MIR4435-2HG OE, which reversed the inhibitory effect of IL-1β. MIR4435-2HG may therefore act as an OA suppressor. In addition, the results from CCK-8 assay demonstrated that MIR4435-2HG OE significantly increased CHON-001 cell proliferation; however, IL-1β significantly inhibited the proliferation of CHON-001 cells (Fig. 3B). Thus, MIR4435-2HG OE reversed the inhibiting effect of IL-1β on cell proliferation. Similarly, the Ki-67-positive rate of CHON-001 cells was significantly decreased by IL-1β, which was reversed by MIR4435-2HG OE (Fig. 3C and D). Furthermore, IL-1β significantly increased CHON-001 cell apoptosis; however, MIR4435-2HG OE inhibited the pro-apoptotic effect of IL-1β treatment on CHON-001 cells (Fig. 3E and F). Taken together, these results indicated that MIR4435-2HG OE may significantly enhance the proliferation of CHON-001 cells following treatment with IL-1β.

MIR4435-2HG OE downregulates MMP1 and MMP13 expression and upregulates collagen II expression in IL-1β-treated CHON-001 cells. Western blotting was used to detect protein expression in CHON-001 cells. MIR4435-2HG OE significantly decreased the expression of MMP1 and MMP13 and upregulated the protein expression of collagen II in IL-1β-treated CHON-001 cells, compared with IL-1β treatment alone (Fig. 4).

MIR4435-2HG OE significantly suppresses the progression of OA via the miR-510-3p/IL-17A axis. To explore the underlying mechanism of MIR4435-2HG in OA progression *in vitro*, Starbase, Targetscan, miRDB predictions were used together with a dual luciferase reporter assay. According to Starbase predictions, miR-510-3p was identified as a potential

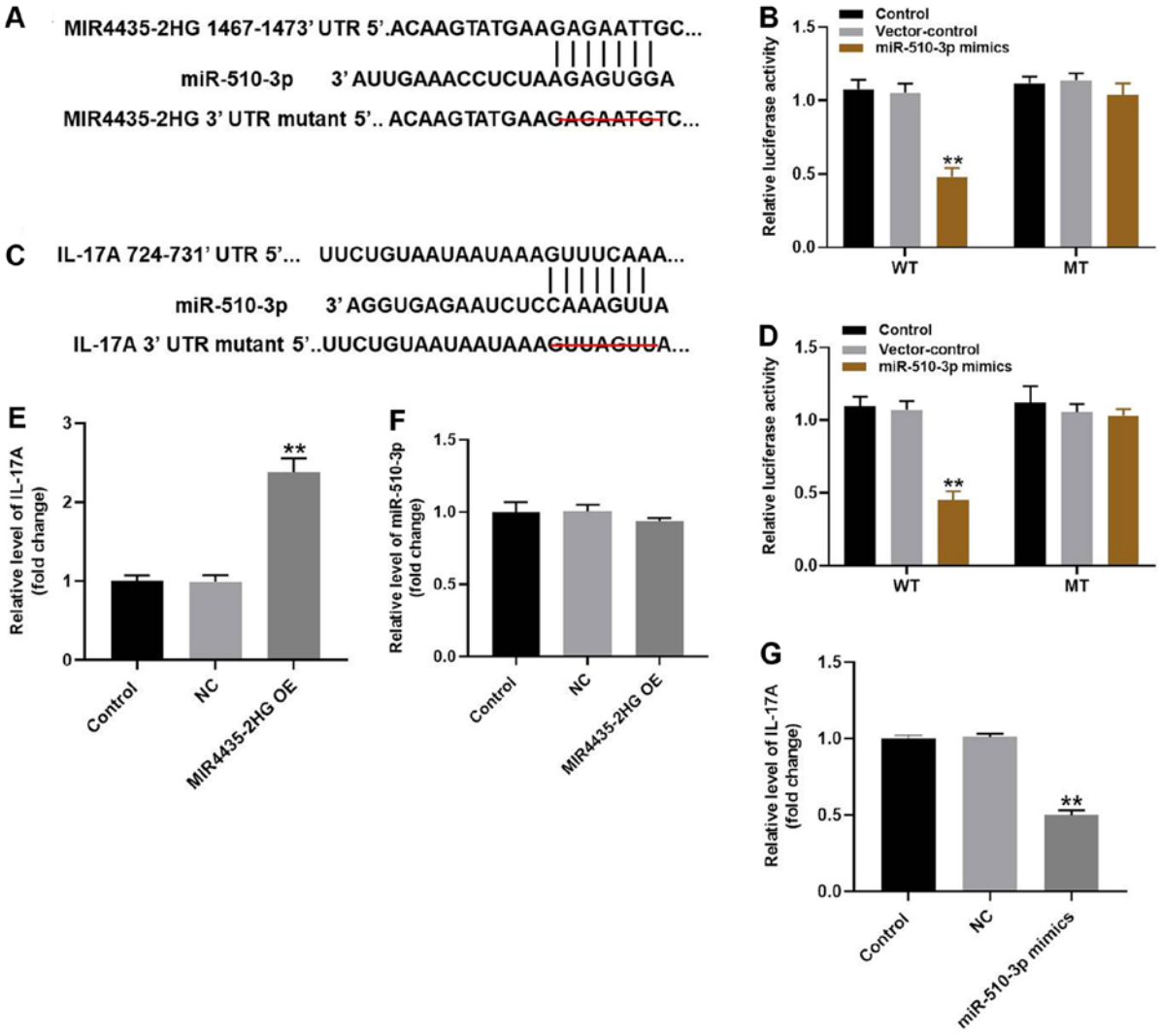

Figure 5. MIR4435-2HG OE significantly suppressed the progression of OA via the miR-510-3p/IL-17A axis. (A) Gene structure of MIR4435-2HG at the position of 1467-1473 indicated the predicted target site of miR-510-3p in its 3'UTR, with a sequence of GACAATC. (B) Luciferase activity was measured in CHON-001 cells following co-transfection with WT/MT MIR4435-2HG 3'-UTR plasmid and miR-510-3p with the dual luciferase reporter assay. (C) Gene structure of IL-17A at the position of 724-731 indicated the predicted target site of miR-510-3p in its 3'UTR, with a sequence of GUUAGUU. (D) Luciferase activity was measured in CHON-001 cells following co-transfection with WT/MT IL-17A 3'-UTR plasmid and miR-510-3p with the dual luciferase reporter assay. (E) Gene expression of IL-17A in CHON-001 cells was detected by RT-qPCR. (F) Gene expression of miR-510-3p in CHON-001 cells was detected by RT-qPCR. (G) Gene expression of IL-17A in CHON-001 cells was detected by RT-qPCR. **P<0.01 vs. control. OE, overexpression; IL, interleukin; miR, microRNA; RT-qPCR, reverse transcription-quantitative PCR; WT, wildtype; MT, mutant; UTR, untranslated region; NC (empty vector), negative control.

downstream target of miR4435-2HG. Furthermore, IL-17A was likely to be a potential target of miR-510-3p according to the Targetscan and miRDB databases (Fig. 5A-D). Since previous studies reported that IL-17A serves a key role in the progression of OA (19,20), IL-17A was also considered as a direct target of miR-510-3p in the present study. The aforementioned results were further verified by RT-qPCR (Fig. 5E). Expression of miR-510-3p was not altered by MI miR4435-2HG OE in CHON-001 cells (Fig. 5F). However, the expression of IL-17A in CHON-001 cells was significantly decreased in the presence of miR-510-3p mimics (Fig. 5G). Taken together, these results suggested that MIR4435-2HG may inhibit OA via the miR-510-3p/IL-17A axis.

MIR4435-2HG OE suppresses OA via regulation of miR-510-3p/IL-17A axis and NF-κB signaling pathway. To further investigate the underlying mechanism of MIR4435-2HG in OA progression, western blotting was performed. The expression of IL-17A in CHON-001 cells was significantly inhibited following treatment with IL-1β, and MIR4435-2HG OE partially reversed IL-1β-mediated effects on IL-17A expression (Fig. 6A and B). MIR4435-2HG OE alone also significantly enhanced the expression of IL-17A in CHON-001 cells. Furthermore, IL-1β significantly increased p-p65 and p-IκB expression in CHON-001 cells. However, IL-1β-induced effects on NF-κB signaling pathway were significantly suppressed by MIR4435-2HG OE (Fig. 6A, C and D). In addition, the NF-κB inhibitor BAY 11-7085 further enhanced the inhibitory effect of MIR4435-2HG OE on NF-κB signaling pathway (Fig. 6E-G). These results demonstrated that MIR4435-2HG OE significantly suppressed the progression of OA via the miR-510-3p/IL-17A axis and by inactivating the NF-κB signaling pathway.

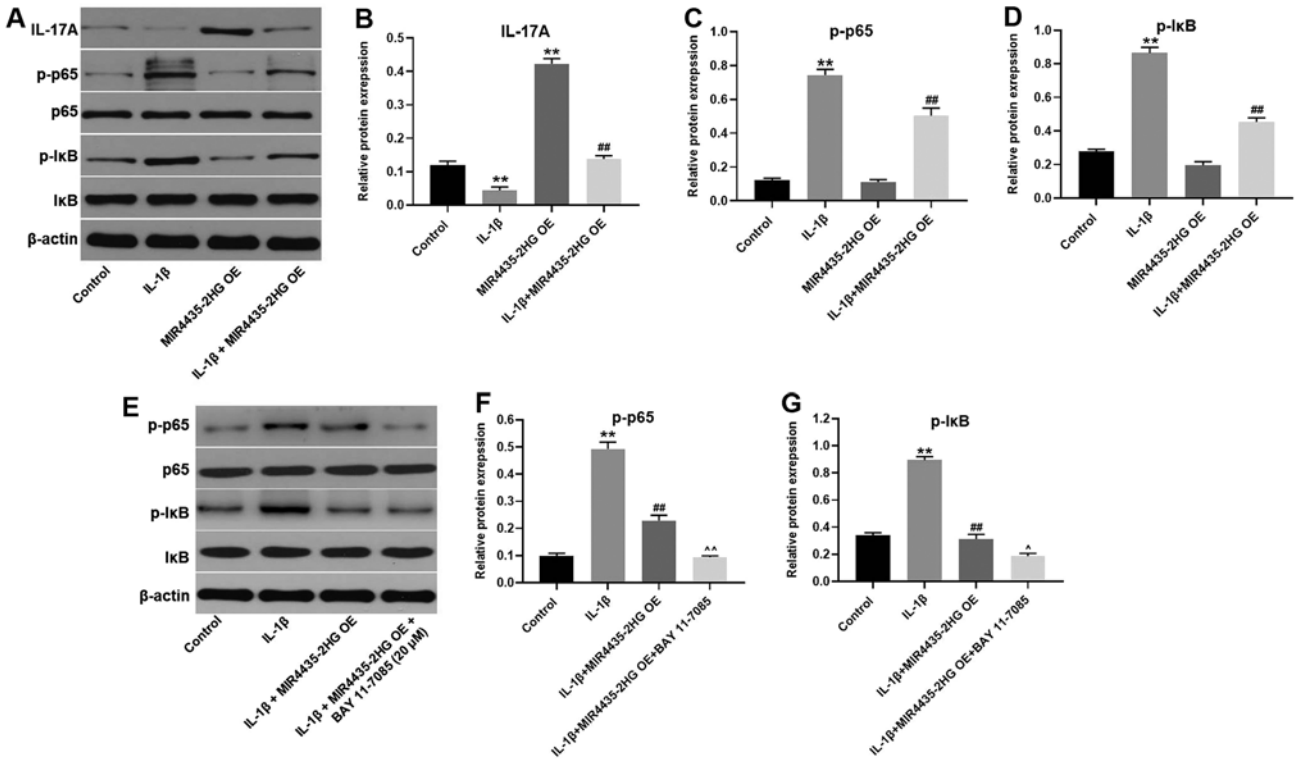

Figure 6. MIR4435-2HG OE suppressed OA progression via the miR-510-3p/IL-17A axis and inactivation of the nuclear factor-κB signaling pathway. CHON-001 cells were treated with IL-1β, MIR4435-2HG OE vector or IL-1β+ MIR4435-2HG OE. Then, (A) protein expression of IL-17A, p-p65, p65, p-IκB and IκB in CHON-001 cells was measured by western blotting. (B) Relative protein expression of IL-17A was normalized to β-actin. (C) Relative protein expression of p-p65 was normalized to p65. (D) Relative protein expression of p-IκB was normalized to IκB. (E) CHON-001 cells were treated with IL-1β, IL-1β+ MIR4435-2HG OE or IL-1β+ MIR4435-2HG OE + BAY-11-7085. Then, protein expression of p-p65, p65, p-IκB and IκB in CHON-001 cells were measured by western blot. (F) Relative protein expression of p-p65 was normalized to p65. (G) Relative protein expression of p-IκB was normalized to IκB. **P<0.01 vs. control; $^{\#\#}$P<0.01 vs. IL-1β; $^{\wedge}$P<0.05, $^{\wedge\wedge}$P<0.01 vs. IL-1β+MIR4435-2HG OE. OE, overexpression; OA, osteoarthritis, miR; microRNA; IL, interleukin; IκB, inhibitor of κB.

Discussion

Previous studies suggested that certain lncRNAs are involved in the pathology of OA (21,22). The present study demonstrated that MIR4435-2HG was significantly downregulated in IL-1β-treated CHON-001 cells. Similarly, Wang *et al* (16) indicated that the expression of lncRNA-recombination signal binding protein for immunoglobulin κ J region (RBPJ, previously known as CBF1) interacting corepressor displayed an inhibitory role during OA progression. In addition, a recent study reported that the inflammatory response plays an important role during the progression of OA (23). Tan *et al* (24) demonstrated that IL-1β serves a key role in the progression of OA. Furthermore, IL-1β enhances injury in arthritic cartilage and increases the expression of matrix-degradation proteins (25). These studies indicated that low expression of MIR4435-2HG was associated with the development of OA.

Collagen II, MMP1 and MMP13 are cartilage matrix components (26,27). Inhibition of collagen II and upregulation of MMP13 and MMP1 could lead to the progression of OA (28-30). In the present study, *in vitro* experiments were performed to further explore the biological role of MIR4435-2HG during OA progression. CHON-001 cell proliferation was inhibited by IL-1β. In addition, MIR4435-2HGOE significantly decreased the expression of MMP1 and MMP13 and increased the expression of collagen II in IL-1β-treated CHON-001 cells. These results were consistent with previous studies indicating that MIR4435-2HG OE attenuates the progression of OA by modulating the expression of MMP1, MMP13 and collagen II.

The mechanism underlying MIR4435-2HG-mediated inhibition of OA progression *in vitro* was also investigated. A dual luciferase reporter assay indicated that miR-510-3p was the downstream target gene of MIR4435-2HG. miRNAs are highly conserved ncRNAs that display versatile biological functions (31-33). Lei *et al* (34) reported that the lncRNA small nucleolar RNA host gene 1 could inhibit IL-1β-induced OA by inhibiting miR-16-5p-mediated p38/MAPK and NF-κB signaling pathway. In addition, the lncRNA metastasis associated lung adenocarcinoma transcript 1 promotes the progression of OA by regulating themiR-150-5p/AKT3 axis (35). However, the function of miR-510-3p in OA remains unclear. The present study demonstrated that miR-510-3p may promote OA progression. These findings were similar to previous studies (36,37), demonstrating that MIR4435-2HG can inhibit the progression of OA by sponging miR-510-3p.

It has been reported that miRNAs exert their function by binding to target genes (38,39). To explore the underlying mechanism of miR-510-3p in the development of OA, the TargetScan database was used for prediction of miR-510-3p target genes, and IL-17A was identified as a direct target of miR-510-3p. IL-17A

is an important immune regulator secreted by Th17 cells (40). It has been reported that IL-17A servesakey role in the pathogenesis of autoimmune diseases (41). In addition, IL-17A deficiency increases susceptibility to multiple diseases through STAT5 phosphorylation (42). In the present study, a luciferase reporter assay also identified IL-17A as a direct target gene of miR-510-3p. In addition, IL-1β treatment significantly decreased the expression of IL-17A in CHON-001 cells, which suggested that IL-17A may act as an OA suppressor. Zhang *et al* (43) reported that IL-17A upregulation could be involved in inflammatory arthritis by acting as an inhibitor, which was similar to the results from the present study, suggesting therefore that IL-17A may be considered as a key regulator during OA. Taken together, the inhibition of IL-1β-induced CHON-001 cell damage occurred by upregulating the expression of IL-17A.

NF-κB signaling is a key regulator in multiple diseases (44,45). NF-κB is an evolutionarily conserved transcription factor that controls the expression levels of various cytokines and adhesion molecules, and is involved in responses to infection, stress and damage (46). p65 is an important downstream protein of NF-κB (47). Activation of NF-κB results in nuclear translocation, which is regulated by the targeted phosphorylation and subsequent degradation of IκB (48). In the present study, MIR4435-2HG OE inactivated NF-κB signaling pathway, suggesting that NF-κB may serve as a promoter during OA. Similar to the findings from the present study, Ren *et al* (49) reported that IL-17A could activate NF-κB signaling pathway, further supporting that MIR4435-2HG may alleviate the progression of OA via IL-17A/NF-κB axis. However, the present study only focused on the association between miR4435-2HG and NF-κB signaling pathway. Since IL-6/STAT3 are involved in the progression of OA (50,51), the effect of MIR4435-2HG on IL-6/STAT3 signaling should be investigated in future studies.

In conclusion, MIR4435-2HG OE significantly inhibited the progression of OA *in vitro*, suggesting that MIR4435-2HG OE may serve as a novel therapeutic strategy for OA.

Acknowledgements

Not applicable.

Funding

No funding was received.

Availability of data and materials

The datasets used and/or analyzed during the current study are available from the corresponding author on reasonable request.

Authors' contribution

YL, YY and LD conceived and supervised the current study. YuqJ and YunJ designed the experiments. YL and LD performed the experiments. All authors read and approved the final manuscript.

Ethics approval and consent to participate

The present study was approved by the Institutional Ethical Committee of the Second Affiliated Hospital of Inner Mongolia Medical University. Written informed consent was obtained from all participants.

Patient consent for publication

Not applicable.

Competing interests

The authors declare that they have no competing interests.

References

1. Thompson RL, Gardner JK, Zhang S and Reinbolt JA: Lower-limb joint reaction forces and moments during modified cycling in healthy controls and individuals with knee osteoarthritis. Clin Biomech (Bristol, Avon) 71: 167-175, 2020.
2. Brandt KD: Osteoarthritis. Clin Geriatr Med 4: 279-293, 1988.
3. Mehl J, Imhoff AB and Beitzel K: Osteoarthritis of the shoulder: Pathogenesis, diagnostics and conservative treatment options. Orthopade 47: 368-376, 2018 (In German).
4. Lukusa A, Malemba JJ, Lebughe P, Akilimali P and Mbuyi-Muamba JM: Clinical and radiological features of knee osteoarthritis in patients attending the university hospital of Kinshasa, Democratic Republic of Congo. Pan Afr Med J 34: 29, 2019.
5. Andreasson I, Kjellby-Wendt G, Fagevik-Olsén M, Aurell Y, Ullman M and Karlsson J: Long-term outcomes of corrective osteotomy for malunited fractures of the distal radius. J Plast Surg Hand Surg 54: 94-100, 2020.
6. Nehrer S, Ljuhar R, Steindl P, Simon R, Maurer D, Ljuhar D, Bertalan Z, Dima HP, Goetz C and Paixao T: Automated knee osteoarthritis assessment increases physicians' agreement rate and accuracy: Data from the osteoarthritis initiative. Cartilage: Nov 24, 2019 (Epub ahead of print).
7. Gerbrands TA, Pisters MF and Vanwanseele B: Individual selection of gait retraining strategies is essential to optimally reduce medial knee load during gait. Clin Biom (Bristol, Avon) 29: 828-834, 2014.
8. Hochberg-Laufer H, Neufeld N, Brody Y, Nadav-Eliyahu S, Ben-Yishay R and Shav-Tal Y: Availability of splicing factors in the nucleoplasm can regulate the release of mRNA from the gene after transcription. PLoS Genet 15: e1008459, 2019.
9. Qi Y, Ma Y, Peng Z, Wang L, Li L, Tang Y, He J and Zheng J: Long noncoding RNA PENG upregulates PDZK1 expression by sponging miR-15b to suppress clear cell renal cell carcinoma cell proliferation. Oncogene: Apr 27, 2020 (Epub ahead of print).
10. Soares JC, Soares AC, Rodrigues VC, Melendez ME, Santos AC, Faria EF, Reis RM, Carvalho AL and Oliveira ON Jr: Detection of the prostate cancer biomarker PCA3 with electrochemical and impedance-based biosensors. ACS Appl Mater Interfaces 11: 46645-46650, 2019.
11. Tu C, Ren X, He J, Zhang C, Chen R, Wang W and Li Z: The Value of LncRNA BCAR4 as a prognostic biomarker on clinical outcomes in human cancers. J Cancer 10: 5992-6002, 2019.
12. Jiang Z, Li L, Hou Z, Liu W, Wang H, Zhou T, Li Y and Chen S: LncRNA HAND2-AS1 inhibits 5-fluorouracil resistance by modulating miR-20a/PDCD4 axis in colorectal cancer. Cell Signal 66: 109483, 2020.
13. Li Y, Li S, Luo Y, Liu Y and Yu N: LncRNA PVT1 regulates chondrocyte apoptosis in osteoarthritis by acting as a sponge for miR-488-3p. DNA Cell Biol 36: 571-580, 2017.
14. Xiao Y, Bao Y, Tang L and Wang L: LncRNA MIR4435-2HG is downregulated in osteoarthritis and regulates chondrocyte cell proliferation and apoptosis. J Orthop Surg Res 14: 247, 2019.
15. Kloppenburg M, Kroon FP, Blanco FJ, Doherty M, Dziedzic KS, Greibrokk E, Haugen IK, Herrero-Beaumont G, Jonsson H, Kjeken I, *et al*: 2018 update of the EULAR recommendations for the management of hand osteoarthritis. Ann Rheumatic Dis 78: 16-24, 2019.
16. Wang X, Fan J, Ding X, Sun Y, Cui Z and Liu W: Tanshinone I inhibits IL-1β-induced apoptosis, inflammation and extracellular matrix degradation in chondrocytes CHON-001 cells and attenuates murine osteoarthritis. Drug Des Devel Ther 13: 3559-3568, 2019.

17. Lin Q and Di YP: Determination and quantification of bacterial virulent gene expression using quantitative real-time PCR. Methods Mol Biol 2102: 177-193, 2020.
18. McAlinden A and Im GI: MicroRNAs in orthopaedic research: Disease associations, potential therapeutic applications, and perspectives. J Orthop Res 36: 33-51, 2018.
19. Lu F, Liu P, Zhang Q, Wang W and Guo W: Association between the polymorphism of IL-17A and IL-17F gene with knee osteoarthritis risk: A meta-analysis based on case-control studies. J Orthop Surg Res 14: 445, 2019.
20. Kaul NC, Mohapatra SR, Adam I, Tucher C, Tretter T, Opitz CA, Lorenz HM and Tykocinski LO: Hypoxia decreases the T helper cell-suppressive capacity of synovial fibroblasts by downregulating IDO1-mediated tryptophan metabolism. Rheumatology 59: 1148-1158, 2020.
21. Lin S, Zhang R, An X, Li Z, Fang C, Pan B, Chen W, Xu G and Han W: LncRNA HOXA-AS3 confers cisplatin resistance by interacting with HOXA3 in non-small-cell lung carcinoma cells. Oncogenesis 8: 60, 2019.
22. Nanus DE, Wijesinghe SN, Pearson MJ, Hadjicharalambous MR, Rosser A, Davis ET, Lindsay MA and Jones SW: Obese osteoarthritis patients exhibit an inflammatory synovial fibroblast phenotype, which is regulated by the long non coding RNA MALAT1. Arthritis Rheumatol 72: 1-29, 2019.
23. Mao T, He C, Wu H, Yang B and Li X: Silencing lncRNA HOTAIR declines synovial inflammation and synoviocyte proliferation and promotes synoviocyte apoptosis in osteoarthritis rats by inhibiting Wnt/β-catenin signaling pathway. Cell Cycle 18: 3189-3205, 2019.
24. Tan C, Zhang J, Chen W, Feng F, Yu C, Lu X, Lin R, Li Z, Huang Y, Zheng L, *et al*: Inflammatory cytokines via up-regulation of aquaporins deteriorated the pathogenesis of early osteoarthritis. PLoS One 14: e0220846, 2019.
25. Kapoor M, Martel-Pelletier J, Lajeunesse D, Pelletier JP and Fahmi H: Role of proinflammatory cytokines in the pathophysiology of osteoarthritis. Nat Rev Rheumatol 7: 33-42, 2011.
26. Zhang Y, Liu S, Guo W, Hao C, Wang M, Li X, Zhang X, Chen M, Wang Z, Sui X, *et al*: Coculture of hWJMSCs and pACs in oriented scaffold enhances hyaline cartilage regeneration in vitro. Stem Cells Int 2019: 5130152, 2019.
27. Wang M, Sampson ER, Jin H, Li J, Ke QH, Im HJ and Chen D: MMP13 is a critical target gene during the progression of osteoarthritis. Arthritis Res Ther 15: R5, 2013.
28. Ji B, Ma Y, Wang H, Fang X and Shi P: Activation of the P38/CREB/MMP13 axis is associated with osteoarthritis. Drug Des Devel Ther 13: 2195-2204, 2019.
29. Zheng W, Feng Z, Lou Y, Chen C, Zhang C, Tao Z, Li H, Cheng L and Ying X: Silibinin protects against osteoarthritis through inhibiting the inflammatory response and cartilage matrix degradation in vitro and in vivo. Oncotarget 8: 99649-99665, 2017.
30. Lorenz J, Seebach E, Hackmayer G, Greth C, Bauer RJ, Kleinschmidt K, Bettenworth D, Böhm M, Grifka J and Grässel S: Melanocortin 1 receptor-signaling deficiency results in an articular cartilage phenotype and accelerates pathogenesis of surgically induced murine osteoarthritis. PLoS One 9: e105858, 2014.
31. Lin SL and Ying SY: Mechanism and method for generating tumor-free ips cells using intronic microRNA miR-302 induction. Methods Mol Biol 1733: 265-282, 2018.
32. Eguchi T and Kuboki T: Cellular reprogramming using defined factors and microRNAs. Stem Cells Int 2016: 7530942, 2016.
33. Pourrajab F, Vakili Zarch A, Hekmatimoghaddam S and Zare-Khormizi MR: The master switchers in the aging of cardiovascular system, reverse senescence by microRNA signatures; as highly conserved molecules. Prog Biophys Mol Biol 119: 111-128, 2015.
34. Lei J, Fu Y, Zhuang Y, Zhang K and Lu D: LncRNA SNHG1 alleviates IL-1beta-induced osteoarthritis by inhibiting miR-16-5p-mediated p38 MAPK and NF-kappaB signaling pathways. Bioscience reports 39, 2019.
35. Zhang Y, Wang F, Chen G, He R and Yang L: LncRNA MALAT1 promotes osteoarthritis by modulating miR-150-5p/AKT3 axis. Cell Biosci 9: 54, 2019.
36. Gao H, Peng L, Li C, Ji Q and Li P: Salidroside alleviates cartilage degeneration through NF-κB pathway in osteoarthritis rats. Drug Des Devel Ther 14: 1445-1454, 2020.
37. Xu C, Sheng S, Dou H, Chen J, Zhou K, Lin Y and Yang H: α-Bisabolol suppresses the inflammatory response and ECM catabolism in advanced glycation end products-treated chondrocytes and attenuates murine osteoarthritis. Int Immunopharmacol: Apr 22, 2020 (Epub ahead of print).
38. Adlakha YK and Saini N: Brain microRNAs and insights into biological functions and therapeutic potential of brain enriched miRNA-128. Mol Cancer 13: 33, 2014.
39. Plé H, Landry P, Benham A, Coarfa C, Gunaratne PH and Provost P: The repertoire and features of human platelet microRNAs. PLoS One 7: e50746, 2012.
40. Wang J, Wang X, Wang L, Sun C, Xie C and Li Z: MiR-let-7d-3p regulates IL-17 expression through targeting AKT1/mTOR signaling in CD4(+) T cells. In vitro Cell Dev Biol Animal 56: 67-74, 2020.
41. Zhou X, Chen H, Wei F, Zhao Q, Su Q, Lei Y, Yin M, Tian X, Liu Z, Yu B, *et al*: α-mangostin attenuates pristane-induced lupus nephritis by regulating Th17 differentiation. Int J Rheum Dis 23: 74-83, 2020.
42. Me R, Gao N, Dai C and Yu FX: IL-17 Promotes pseudomonas aeruginosa keratitis in C57BL/6 mouse corneas. J Immunol 204: 169-179, 2020.
43. Zhang X, Yuan Y, Pan Z, Ma Y, Wu M, Yang J, Han R, Chen M, Hu X, Liu R, *et al*: Elevated circulating IL-17 level is associated with inflammatory arthritis and disease activity: A meta-analysis. Clin Chim Acta 496: 76-83, 2019.
44. Ghosh S, May MJ and Kopp EB: NF-kappa B and Rel proteins: Evolutionarily conserved mediators of immune responses. Ann Rev Immunol 16: 225-260, 1998.
45. Puri RV, Yerrathota S, Home T, Idowu JY, Chakravarthi VP, Ward CJ, Singhal PC, Vanden Heuvel GB, Fields TA and Sharma M: Notch4 activation aggravates NF-κB mediated inflammation in HIV-1 associated Nephropathy. Dis Mod Mech 12: pii: dmm040642, 2019.
46. Baldwin AS Jr: The NF-kappa B and I kappa B proteins: New discoveries and insights. Ann Rev Immunol 14: 649-683, 1996.
47. Schütze S, Wiegmann K, Machleidt T and Krönke M: TNF-induced activation of NF-kappa B. Immunobiology 193: 193-203, 1995.
48. TH, Lv MM, An XM, Leung WK and Seto WK: Activation of adenosine A3 receptor inhibits inflammatory cytokine production in colonic mucosa of patients with ulcerative colitis by down-regulating the NF-kappaB signaling. J Dig Dis 21: 38-45, 2020.
49. Ren H, Wang Z, Zhang S, Ma H, Wang Y, Jia L and Li Y: IL-17A promotes the migration and invasiveness of colorectal cancer cells through NF-κB-mediated MMP expression. Oncol Res 23: 249-256, 2016.
50. Sui C, Zhang L and Hu Y: MicroRNA-let-7a inhibition inhibits LPS-induced inflammatory injury of chondrocytes by targeting IL6R. Mol Med Rep 20: 2633-2640, 2019.
51. Lu W, Ding Z, Liu F, Shan W, Cheng C, Xu J, He W, Huang W, Ma J and Yin Z: Dopamine delays articular cartilage degradation in osteoarthritis by negative regulation of the NF-kappaB and JAK2/STAT3 signaling pathways. Biomed Pharmacother 119: 109419, 2019.